THE ASTROPHYSICAL JOURNAL, 386:181–189, 1992 February 10

HYDROGEN RECOMBINATION AT HIGH OPTICAL DEPTH AND THE SPECTRUM OF SN 1987A

YUEMING XU
School of Natural Sciences, Institute for Advanced Study, Princeton, NJ 08540

RICHARD MCCRAY
Joint Institute for Laboratory Astrophysics, University of Colorado, Boulder, CO 80309-0440

ERNESTO OLIVA AND SOFIA RANDICH
Osservatorio Astrofisico Arcetri, Largo Enrico Fermi 5, I-50125 Firenze, Italy
Received 1991 May 6; accepted 1991 August 19

ABSTRACT

We describe a general theory for hydrogen recombination line formation in an expanding medium in which some of the lines are optically thick. With this theory we calculate the time evolution of the hydrogen lines of SN 1987A at $t \gtrsim 150$ days, assuming that the supernova envelope is a homologously expanding uniform sphere. The theoretical luminosities and ratios of the recombination lines agree remarkably well with the observations. For the first 2 yr, the supernova envelope is optically thick to Balmer continuum. For $t \lesssim 400$ days, hydrogen is ionized primarily from the $n = 2$ level by Balmer continuum photons, which are provided partly by the two-photon decay of the $2s$ state and partly by emission lines of heavy elements. The ionization fraction in the envelope varies slowly ($t \lesssim 400$ days), with $N_e/N_H \approx 10^{-2}$, and decreases exponentially at later times. One unsolved puzzle remains: the luminosity of Hα is systematically weaker by a factor of ~ 2 than the value we expected from the luminosity of the infrared recombination lines.

Subject headings: ISM: individual (SN 1987A) — line: formation — stars: individual (SN 1987A) — supernovae: individual (SN 1987A)

1. INTRODUCTION

For the first 3 months after outburst, the spectrum of SN 1987A resembled a 5000 K blackbody continuum, with strong P Cygni lines indicating rapidly outflowing material above the photosphere; but by $t \approx 5$ months the photosphere had vanished and the spectrum had changed into a nebular spectrum with a weak continuum and strong emission lines. The optical spectrum was dominated by Hα, [Ca II] λ7300, and C II λ8700 emission lines (cf. Phillips & Williams 1991), and the infrared spectrum was dominated by many recombination lines of hydrogen, several forbidden lines of neutral and singly ionized trace elements, and CO and SiO emission bands (cf. Wooden 1989). The bolometric luminosity of SN 1987A at $t = 9$ months was distributed roughly as follows: 15% hydrogen recombination lines; 5% other emission lines; 80% continuum. The continuum luminosity was concentrated mainly in the blue, and it is not clear whether it is a true continuum or a blend of many overlapping emission lines.

The optical and infrared spectra have remained qualitatively similar even since. Ratios of forbidden lines indicate that the envelope of SN 1987A is remarkably cold, $T \lesssim 3500$ K, throughout (Oliva, Moorwood, & Danziger 1989; Varani et al. 1990). At such temperatures, thermal electrons can excite the observed optical and infrared emission lines of trace elements, but they cannot ionize the hydrogen. It is clear that the hydrogen ionization and heating of the envelope result from the reprocessing of the luminosity of gamma rays and positrons emitted by ^{56}Co in a medium that is transparent in the optical and infrared continua. By analyzing the nebular spectrum, we hope to infer the physical conditions (density, temperature, composition) within the expanding envelope of SN 1987A, just as we do for other emission line sources such as H II regions and planetary nebulae.

At second glance one notices striking differences between the spectrum of SN 1987A and the spectra of other emission nebulae, the most obvious of which is that there is no Hβ emission despite the strong Hα emission line. Evidently, something new is going on. The essential clues are provided by the absorption feature on the blue side of Hα, and absorption lines at the higher Balmer lines, Hβ, Hγ, etc. These tell us that the higher Balmer lines are optically thick, and so Hβ photons are resonantly trapped and split into Hα and Paα, etc., just as Lyβ is split into Lyα and Hα in a typical nebula. This interpretation is corroborated by the strong O I λ1.129 μm emission line in the infrared spectrum. This line is pumped by resonance fluorescence between O I and Lyβ, a mechanism that requires substantial optical depth in Hα to be efficient (Grandi 1980).

In this paper we show what can be learned about the interior conditions of SN 1987A from interpretation of its hydrogen recombination line spectrum. To do this, we first (§ 2) describe the general theory for recombination line formation in an expanding medium in which some of the lines are optically thick. Then, in § 3, we use this theory to interpret the time evolution of the spectrum of SN 1987A, and we conclude in § 4 with a discussion of the unresolved issues.

2. RECOMBINATION SPECTRUM FORMATION IN AN OPTICALLY THICK MEDIUM

Here we describe the formation of the hydrogen recombination line spectrum in a medium in which some of the Balmer and higher series lines may be optically thick. The description of line transfer is particularly simple for a supernova because the envelope dynamics is known. After several days (2 weeks at most), we can be confident that pressure forces are negligible in the supernova envelope, so that any comoving element of gas is in free hypersonic expansion. By 3 months, it is a good approximation to say that any comoving element of gas (with radial velocity v) has a radius given by $r = vt$, where t is the

time since the explosion, and a density given by $\rho(r, t) = (t/t_0)^{-3}\rho(r_0, t_0)$, where $r_0 = vt_0$ and t_0 is any other time. Thus, the relative velocities of any atoms in the supernova envelope obey a Hubble law, $\Delta v = H(t)\Delta r$, where the "Hubble constant" $H(t) = t^{-1}$.

2.1. *Line Trapping and Escape Probability*

Such an environment provides the simplest case for describing the trapping of spectral lines. Because the expansion is hypersonic, we can use the Sobolev approximation (Sobolev 1960; Castor 1970; Mihalas 1978). At any given frequency, the emitting region for a given spectral line is confined to a thin planar section (the surface moving with constant projected Doppler velocity $\Delta v = c\,\Delta\nu/\nu_0$) through the supernova envelope. The fractional thickness of the section given by $\delta z/z \approx v_{\rm th}/\Delta v$, where $v_{\rm th} = (2kT/m)^{1/2} = 4.06(T_3/A)^{1/2}$ km s^{-1} is the molecular speed in the gas and $\Delta v \leq v_{\rm max} \sim$ 1000–2500 km s^{-1} is the expansion velocity seen in the line profiles. For such an environment, the Sobolev optical depth of the line assumes the simple form,

$$\tau = \frac{\pi e^2}{m_e c} f_{lu}\lambda_0 t N_l\left[1 - \frac{g_l N_u}{g_u N_l}\right] = \frac{\lambda_0^3 t g_u A_{ul} N_l}{8\pi g_l}\left[1 - \frac{g_l N_u}{g_u N_l}\right], \quad (1)$$

where f_{lu} is the oscillator strength for the absorption line, A_{ul} is the radiative decay rate for the corresponding line emission, λ_0 is the rest wavelength of the line, N_l, g_l, N_u, g_u are the atomic number density and statistical weights of the lower and upper states, respectively, and the square brackets account for induced emission.

Then, according to Sobolev theory, the probability that a line photon will escape from the scattering layer is given by

$$P_{\rm esc}(\tau) = \tau^{-1}[1 - \exp(-\tau)], \quad (2)$$

and the local line emissivity is given by

$$j_\nu = \frac{h\nu_0}{4\pi} N_u A_{ul} P_{\rm esc}\,\phi(\Delta\nu), \quad (3)$$

where the line profile function has the property $\int \phi(\Delta\nu)d(\Delta\nu) = 1$. The specific intensity at a given frequency is then given by

$$I_\nu = \int dz j_\nu = \frac{h\nu_0}{4\pi} N_u A_{ul} P_{\rm esc}\frac{ct}{\nu_0}, \quad (4)$$

where we have used the Doppler formula $d(\Delta\nu) = \nu_0\, dv_z/c = \nu_0\, dz/ct$. From equations (1), (2), and (4), we find the reasonable result that for $\tau \gg 1$, $I_\nu \rightarrow B_\nu(T_{ul})$ (the Planck function), where T_{ul} is the excitation temperature, $N_u/N_l = (g_u/g_l)\exp(-h\nu/kT_{ul})$.

Resonant trapping reduces the effective radiative decay rate A_{ul} by the factor $P_{\rm esc}$. If the line optical depth is great enough, so that $P_{\rm esc} \ll 1$, resonance line transitions will act like forbidden transitions. For example, the density of atomic hydrogen in the envelope of SN 1987A at $t = 1$ yr is $N_{\rm H} \sim 3 \times 10^9$ cm^{-3}. Then, according to equation (1), the optical depth in Lyα is $\tau(\text{Ly}\alpha) \sim 10^{10}$, so the effective rate for the $2P$ state to decay by Lyα emission is $A_{2,1}/\tau(\text{Ly}\alpha) \sim 0.05$ s^{-1}. Thus the $n = 2$ level of hydrogen becomes "metastable," and its lifetime is determined by two-photon decay ($A_{2\gamma} = 2.05$ s^{-1}, assuming complete l mixing of the $n = 2$ level) and by de-excitation by thermal electrons rather than by Lyα decay.

As we shall show, in the envelope of SN 1987A the population of the $n = 2$ level of hydrogen is so great that the Balmer lines are optically thick for $t \lesssim 2$ yr. If so, Hβ and the higher. Balmer lines will be resonantly trapped and will scatter many times before they escape the resonance scattering layer. The levels of $n = 4$, 5, 6, etc. will decay through branches such as H$\beta \rightarrow$ Hα + Paα, H$\gamma \rightarrow$ Hα + Paβ, H$\gamma \rightarrow$ Hβ + Br$\alpha \rightarrow$ Hα + Paα + Brα, and so forth. Moreover, if the Balmer continuum is optically thick, recombinations directly to the $n = 2$ level will not count because the resulting Balmer continuum photons will be absorbed on the spot. We call the resulting recombination spectrum "case C," extending the terminology of "case A" (Lyman series optically thin) and "case B" (Lyman series optically thick) recombination (cf. Osterbrock 1989). Likewise, "case D" should correspond to the case where the Paschen series becomes optically thick, and so on. (Note that our definition of case C differs from that introduced by Aller, Baker, & Menzel 1939. According to their terminology, case C corresponds to a nebula transparent to Lyman line radiation but with a central star radiating like a blackbody in the region of the Lyman lines.)

2.2. *Ionization and Excitation by Fast Electrons*

Since excitation or ionization of hydrogen atoms from the ground state by thermal electrons is impossible at the low temperatures of the envelope of SN 1987A, we can be sure that excitations and ionizations are caused in the first instance by nonthermal electrons resulting from the degradation of gamma rays from ^{56}Co decay. The energy deposition by nonthermal electrons into ionization, excitation, and heating of hydrogen gas has been calculated in detail by Shull & van Steenberg (1985) and by Xu & McCray (1991a). The main results may be summarized as follows. First, we define a parameter U (eV s^{-1}) to be the rate of energy deposition by fast electrons per hydrogen atom. We also define a parameter Γ (s^{-1}) to characterize the rate per hydrogen atom of ionization plus excitation by nonthermal electrons. Then, we have

$$\Gamma(x) \approx \frac{U}{11.8\text{ eV}}[1 - \eta_h(x)], \quad (5)$$

where $x = N_e/N_{\rm H}$. The function $\eta_h(x)$ gives the fraction of the energy deposition rate U that goes to heating electrons by thermal collisions; it is tabulated by Xu & McCray (1991a). Typical values are $\eta_h(x) = 0.11$, 0.15, 0.26, and 0.57 for $x = 10^{-4}$, 10^{-3}, 10^{-2} and 10^{-1}, respectively. The rate Γ is distributed among bound n states and continuum according to the fractions $f_2 = 0.47$ and $f_C = 0.39$, with the remainder going to states $n > 2$. Thus, it costs at least 34 eV for each ionization directly from the ground state by fast electrons.

Neglecting ionizations or excitations by thermal electrons, the equation for stationary population of the ground state of hydrogen is

$$\Gamma N_{\rm H} = N_2[A_{2\gamma} + N_e C_{2,1}(T) + A_{2,1}/\tau_{2,1}], \quad (6)$$

where $C_{2,1}(T)$ is the rate coefficient for de-excitation of the $n = 2$ level by thermal electrons, $A_{2,1} = 4.696 \times 10^8$ s^{-1} is the effective decay rate for the Lyα transition (assuming complete l mixing), and $\tau_{2,1}$ is the Lyα optical depth (eq. [1]). Equation (6)

can be written

$$\frac{N_2}{N_H} = \frac{\Gamma}{A_{2\gamma}}\left(1 + \frac{N_e}{N_{e,cr}} + \frac{N_{H,cr}}{N_H}\right)^{-1}, \quad (7)$$

where $N_{e,cr} = A_{2\gamma}/C_{2,1} = 1.54 \times 10^8$ cm^{-3} at $T = 3000$ K, $N_{H,cr} = 5.4 \times 10^7 t_y^{-1}$ cm^{-3}, and t_y is the time in years. Then, given N_2 from equation (7), we can calculate the optical depth in Hα from equation (1):

$$\tau_{3,2} = 5.44 \times 10^{-7} \Gamma N_H t\left(1 + \frac{N_e}{N_{e,cr}} + \frac{N_{H,cr}}{N_H}\right)^{-1}. \quad (8)$$

We express the fact that the population of the $n = 2$ level is stationary with the equation:

$$N_1[A_{2\gamma} + N_e C_{2,1}(T) + A_{2,1}/\tau_{2,1} + \zeta_{2,C}] = N_e N_+ \alpha_{eff}(T) + N_H \Gamma f_2, \quad (9)$$

where $\alpha_{eff}(T)$ is the net effective rate coefficient for radiative recombination into $n = 2$ including cascades from all higher states. In equation (9) we have included a term $\zeta_{2,C} = \int J_{BaC}(\lambda)\sigma_{2,C}(\lambda)d\lambda$ to account for photoionization of the $n = 2$ level by Balmer continuum photons [photon mean intensity $J_{BaC}(\lambda)$ cm^{-2} s^{-1} Å^{-1}].

From equation (9) we derive an expression for the emission measure, EM $= \int N_e N_+ dV$:

$$\mathrm{EM} = \frac{\Gamma M_H}{\alpha_{eff}(T) m_H}\left[1 - f_2 + \frac{\zeta_{2,C}}{A_{2\gamma}}\left(1 + \frac{N_e}{N_{e,cr}} + \frac{N_{H,cr}}{N_H}\right)^{-1}\right], \quad (10)$$

where M_H/m_H is the total number of hydrogen atoms that are exposed to nonthermal electrons.

Suppose that the Balmer series and continuum are optically thick and the Paschen series is optically thin (case C). Then the only way for a hydrogen atom to enter the $n = 2$ state is by the emission of Hα (electron impact de-excitation of the $n = 3$ state is always negligible), and we can write

$$N_e N_+ \alpha_{eff}(T) = N_3 A_{3,2}/\tau_{3,2}. \quad (11)$$

For this case, α_{eff} is the net effective recombination rate into all states $n \geq 3$. Using equation (1) to express N_2 and N_3 in terms of $\tau_{3,2}$ and $\tau_{4,3}$, we find from equations (9) and (11) the optical depth in Paα:

$$\tau_{4,3} = 1.747 \times 10^{-7} \times \left[(1 - f_2)\left(1 + \frac{N_e}{N_{e,cr}} + \frac{N_{H,cr}}{N_H}\right) + \frac{\zeta_{2,C}}{A_{2\gamma}}\right]\tau_{3,2}^2. \quad (12)$$

Likewise, one finds that if the Paschen series is optically thick, the equation for stationary population of the $n = 3$ level implies that the Brα optical depth obeys the law $\tau_{5,4} \propto \tau_{3,2}^3$, and so forth.

2.3. *Optically Thick Recombination Line Theory*

In order to calculate the level populations for hydrogen recombination, we assumed complete l mixing and used the method described by Brocklehurst (1971), with the replacement $A_{n,n'} \rightarrow A_{n,n'} P_{esc}(\tau_{n,n'})$ to account for suppression of radiative transitions by line trapping. We used collisional and radiative transition rates provided by Johnson (1972).

The Balmer continuum ionization rate, $\zeta_{2,C}$, was calculated by assuming that the Balmer continuum photons are provided entirely by the two-photon decays of the $n = 2$ level (Nussbaumer & Schmütz 1984), a fraction $0.71[1 - P_{esc}(\tau_{2,C})]$ of which are absorbed (71% of the two-photon continuum lies in the Balmer continuum). We used an expression for the average continuum escape probability given in Appendix 2 of Osterbrock (1989):

$$P_{esc}(\tau) = \frac{3}{4\tau}\left[1 - \frac{1}{2\tau^2} + \left(\frac{1}{\tau} + \frac{1}{2\tau^2}\right)e^{-2\tau}\right]. \quad (13)$$

The continuum optical depth is given by

$$\tau_{nc}(\nu) = \sigma_n(\nu) N_n v_{max} t, \quad (14)$$

where $\sigma_n(\nu)$ is the cross section for photoionization for level n by the photons of frequency ν (Seaton 1959), v_{max} is the expansion velocity of the supernova envelope, and $n = 2$ for Balmer continuum. Note that if the Balmer continuum is optically thick, the effective ionization rate due to fast electrons is increased by a factor 3.2. That occurs because for every ionization directly from the ground state, there are 1.56 excitations to bound states, each of which leads to 1.42 Balmer continuum photons that can ionize H*($n = 2$). Allowing for this extra ionization, it costs at least 10.6 eV for each ionization of hydrogen by nonthermal electrons.

The results are shown in Figure 1. The upper panel shows the effective emissivities ϵ_l (allowing for escape probabilities), and the lower panel shows the optical depths of several selected recombination lines and continua as functions of the Hα optical depth, $\tau(\mathrm{H}\alpha) = \tau_{3,2}$. For the model illustrated, we assumed that the electron density and temperature had constant values of $n_e = 10^8$ cm^{-3} and $T = 3000$ K, respectively.

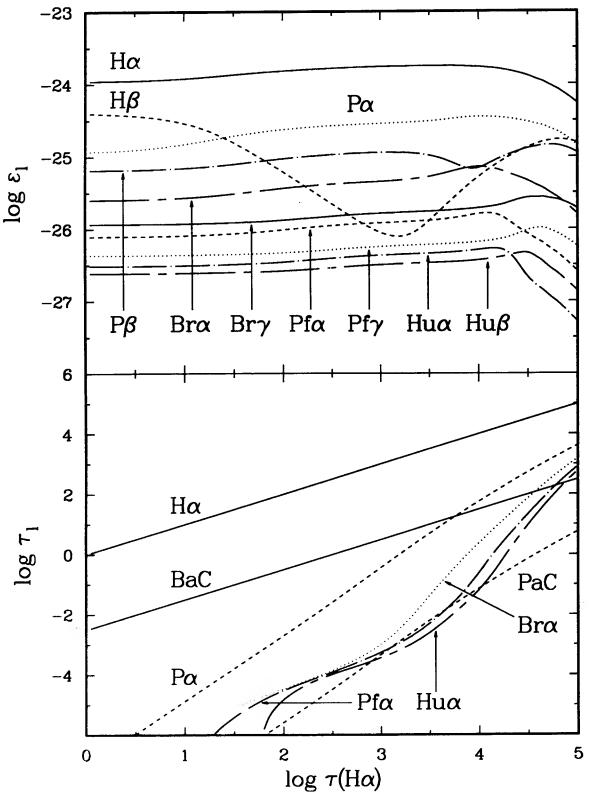

FIG. 1.—Hydrogen recombination lines. *Upper panel*: line emissivities (ergs cm^3 s^{-1}). *Lower panel*: optical depth of recombination lines and continua.

We assumed $v_{max} = 2500$ km s^{-1} for calculating the optical depths of continua.

The results may be understood as follows. When $\log \tau(\mathrm{H}\alpha) \ll 1$, H$\beta$ and all other recombination lines in the Balmer, Paschen, etc., series are optically thin, and the results correspond to case B. The emissivities are listed in Table 1. Note that these numbers differ significantly from those listed in Table 4.4 of Osterbrock (1989), which are valid for low electron density, but they agree within a few percent with the results of Hummer & Storey (1987) for $n_e = 10^8$ cm^{-3}, $T = 3000$ K (listed in the first row of Table 1), for which conditions our approximation of complete l mixing is good. However, with increasing optical depth, $\log \tau(\mathrm{H}\alpha) \gtrsim 1$, H$\beta$ begins to split into Hα + Paα and so its emissivity is suppressed. As this happens, we see a slight rise in the emissivities of the infrared recombination lines owing to the splitting of the higher Balmer lines. For $1 \lesssim \log \tau(\mathrm{H}\alpha) \lesssim 3.5$, the line emissivities are fairly constant, and correspond approximately to case C recombination (Balmer lines optically thick, Paschen and higher lines optically thin). The case C emissivities are also listed in Table 1.

According to equation (12), $\tau(\mathrm{Pa}\alpha) \propto \tau(\mathrm{H}\alpha)^2$, and this behavior is evident in the lower panel of Figure 1. When $\tau(\mathrm{Pa}\alpha) \gtrsim 1$, the Pa$\alpha$ decay is suppressed, and this in turn suppresses the channel H$\beta \rightarrow$ Hα + Paα. Thus, we see that the emissivity of Hβ begins to increase for $\log \tau(\mathrm{H}\alpha) \gtrsim 3$. Then, when $\log \tau(\mathrm{H}\alpha) \gtrsim 3.5$, the emissivity of Pa$\beta$ drops and that of Brα rises as Pa$\beta \rightarrow$ Paα + Brα. This event signifies the onset of "case D" (Paschen series optically thick, Brackett and higher series thin). This idealization is never realized, however. When $\log \tau(\mathrm{H}\alpha) \gtrsim 4.3$, all the higher recombination lines begin to become optically thick, suppressing the entire radiative cascade and the emissivities of all the recombination lines. This marks the approach to local thermodynamic equilibrium.

3. THE RECOMBINATION SPECTRUM OF SN 1987A

3.1. *Model and Assumptions*

Since the recombination line profiles (e.g., Phillips & Williams 1991) are not flat-topped, we infer that the hydrogen is mixed throughout the line emitting region, right down to the center of the supernova envelope. We assume approximate spherical symmetry, so that the volume of the emitting region is given by $V = 4\pi/3(v_{max}t)^3$, where the radial velocity of the emitting region is related to FWHM of the lines by $v_{max} = 2^{-1/2}v_{FWHM}$ if the hydrogen is distributed uniformly throughout the region (in which case the line profile is a parabola). The observed widths of hydrogen lines show that $v_{max} \sim 2500$ km s^{-1} (Miekle et al. 1989). The mixing is probably the result of dynamical instabilities during the explosion (cf. Nomoto et al. 1991), and so we expect that the hydrogen is actually distributed inhomogeneously within this volume with a filling factor f_H. The whole system is expanding freely. Assuming that the hydrogen density is otherwise uniform (an oversimplification, to be sure), we find that the number density of hydrogen atoms in the emitting region is given by

$$N_H = 5.8 \times 10^8 \text{ cm}^{-3} f_H^{-1} \left(\frac{M_H}{M_\odot}\right)\left(\frac{v_{max}}{2500 \text{ km s}^{-1}}\right)^{-3} t_y^{-3} . \quad (15)$$

Note that M_H is only the mass of hydrogen that is contained in the region where the gamma rays deposit most of their energy and does not include the faster moving hydrogen in the outer envelope.

We write the energy deposition per hydrogen atom (cf. eq. [5]) as

$$U = L_\gamma \kappa \frac{m_H}{M_H} = 4.2 \times 10^{-4} f(t) \exp\left(-\frac{t_y}{0.305}\right)\kappa\left(\frac{M_H}{M_\odot}\right)^{-1} \text{eV s}^{-1} , \quad (16)$$

where L_γ is the lumonosity due to ^{56}Co decay that is deposited in the envelope of SN 1987A and κ is the fraction of the gamma-ray luminosity that is absorbed by hydrogen. Since the energy deposition per unit mass is roughly proportional to Z/A, we estimate that $\kappa \approx [1 + M_A/(2M_H)]^{-1} \approx 0.5$, where M_A is the mass of all elements other than hydrogen, and we use the chemical abundances of the Model 10H by Woosley (1988). The function $f(t)$ accounts for the direct escape of hard X-rays and gamma rays; a fit to the ultraviolet, optical, and infrared (UVOIR) luminosity gives (Xu 1989)

$$f(t) = \begin{cases} 1 , & t < 300 \text{ days} \\ 1 - \dfrac{1}{18.5}\left[\left(\dfrac{t}{300^d}\right)^2 - 1\right]^3 , & t > 300 \text{ days} . \end{cases} \quad (17)$$

Given the density and energy deposition rate, we can then use the optically thick recombination theory to determine the ionized fraction, emission measure, and emissivities of all the recombination lines in the envelope. To do this, we must set two additional parameters. The first is the temperature of the envelope, which we assume to be $T = 3000$ K, independent of time. The second is the parameter $\zeta_{2,C}$ describing the rate of photoionization by Balmer continuum. We write

$$\zeta_{2,C} N_2 = (1.42 N_2 + \xi_{2,C} \Gamma N_H)[1 - P_{esc}(\tau_{2,C})] , \quad (18)$$

where the first term represents the Balmer continuum photoionization due to the two-photon decay of the $n = 2$ level and the second term represents the effect of an additional source of Balmer continuum photons, assumed to be proportional to the

TABLE 1

INTENSITIES OF THE RECOMBINATION LINES: $N_e = 10^8$ cm^{-3}, $T = 3000$ K

$\tau(\mathrm{H}\alpha)$	$\epsilon(\mathrm{Pa}\beta)$[a]	Hα/Paβ	Hβ/Paβ	Paα/Paβ	Brα/Paβ	Brγ/Paβ	Pfγ/Paβ	Huα/Paβ
Case B	6.91 (−26)	1.66 (1)	5.99	1.95	4.51 (−1)	1.81 (−1)	6.83 (−2)	5.26 (−2)
0.01	6.43 (−26)	1.68 (1)	6.37	1.76	3.88 (−1)	1.81 (−1)	6.71 (−2)	4.76 (−2)
1	6.48 (−26)	1.69 (1)	6.11	1.81	3.88 (−1)	1.80 (−1)	6.66 (−2)	4.72 (−2)
100	9.40 (−26)	1.61 (1)	6.63 (−1)	2.52	3.88 (−1)	1.40 (−1)	4.96 (−2)	3.68 (−2)
1000	1.14 (−25)	1.52 (1)	7.86 (−2)	2.51	3.96 (−1)	1.44 (−1)	4.98 (−2)	3.77 (−2)
5000	8.56 (−26)	2.06 (1)	2.66 (−1)	3.81	7.04 (−1)	2.09 (−1)	7.18 (−2)	5.47 (−2)
10000	6.90 (−26)	2.47 (1)	7.51 (−1)	5.10	1.04	2.78 (−1)	9.45 (−2)	7.35 (−2)

[a] Ergs cm^3 s^{-1}.

primary ionization rate, $\Gamma N_{\rm H}$. (Note that the Balmer continuum deep inside the supernova envelope may be much greater than the Balmer continuum that emerges from the supernova, owing to strong absorption by resonance fluorescence of ions such as Fe II in the envelope [Xu & McCray 1991b]).

We find that the Paschen continuum is also optically thick at early times, and in that case we include the photoionization from the $n = 3$ level by Hα photons. Each such photoionization effectively removes two Hα photons from the emergent spectrum—the one that is absorbed, and also the one that is lost because the cascade into $n = 3$ is not followed by Hα emission.

3.2. *Results*

Our results are shown in Figures 2–6 for three representative models. For each model, we take $T = 3000$ K, $M_{\rm H} = 5\ M_\odot$, $\kappa = 0.5$, and $f_{\rm H} = 1$. The remaining parameters are $v_{\rm max}$, the expansion velocity of the emitting region, and $\xi_{2,C}$, the measure of the Balmer continuum photoionization. In model 1 (*solid curves*), $v_{\rm max} = 2500$ km s^{-1} and $\xi_{2,C} = 2$; in model 2 (*dashed curves*), $v_{\rm max} = 1500$ km s^{-1} and $\xi_{2,C} = 0$; and in model 3 (*dotted curves*), $v_{\rm max} = 3500$ km s^{-1} and $\xi_{2,C} = 0$.

Figure 2 shows the emission measure calculated for each model (cf. eq. [10]). Also shown are the emission measures inferred from the luminosities of the observed recombination lines. The observed luminosities were calculated by assuming a distance 50 kpc and were corrected for interstellar absorption. They were not, however, corrected for absorption due to dust that formed within the supernova envelope at $t \approx 550$ days (Danziger et al. 1991; Dwek 1991). After that time, the observed values must be regarded as lower limits to the actual emitted luminosity.

To infer the emission measure from the observation, we used the line emissivities ϵ_l, for $N_e = 10^8$ cm^{-3}, $T = 3000$ K, and $\tau(\text{H}\alpha) = 1000$ given in Table 1. Let F_l be the fraction of the UVOIR bolometric luminosity observed in line l (cf. Phillips & Williams 1991). Then, the emission measure derived from this line can be written

$$(\text{EM})_l = \frac{F_l}{\epsilon_l} L_\gamma f(t) \, . \tag{19}$$

Since both the theoretical results and the values inferred from observations scale as the same power of the assumed temperature, $\text{EM} \propto 1/\alpha^{(2)}(T) \propto T^{0.9}$, the comparison between theory and experiment is insensitive to the assumed temperature. The results are insensitive to the assumed value of $M_{\rm H}$, as can be seen from equations (5)–(10), (15), (16), and (18).

We may draw three important conclusions from Figure 2. First, the agreement between theory and observation is remarkably good. For example, model 1 agrees with the observations within the dispersion of the data. That is good evidence that the hydrogen ionization is caused by nonthermal electrons from gamma-ray energy deposition. Second, some extra source of Balmer continuum photons comparable to the two-photon continuum is required for the model to agree with the observed emissions of the infrared recombination lines. No model with $\xi_{2,C} = 0$ can give satisfactory agreement with observation. Third, the emission measures inferred from the Hα line observations are systematically low (by factors ~ 2) compared to those inferred from the infrared recombination lines. We have not found a satisfactory explanation for this fact (cf. § 4).

Figure 3 shows the factional ionization of hydrogen for the three models. The results are directly related to those of Figure 2 through $N_e/N_{\rm H} \propto (\text{EM})^{1/2} M_{\rm H}^{-1} (v_{\rm max}\, t)^{3/2}$ and are therefore sensitive to the assumed values of $v_{\rm max}$ and $M_{\rm H}$. The fractional ionization does not decrease for early times ($t \lesssim 300$ days) because the density of hydrogen atoms is decreasing faster than Γ.

Figure 4 shows the optical depth $\tau(\text{H}\alpha)$ for the three models (cf. eq. [8]). The results are insensitive to the assumed value of $M_{\rm H}$, but they do depend on $v_{\rm max}$: $\tau(\text{H}\alpha) \propto v_{\rm max}^{-3}$. The solid and dashed curves flatten out because $N_e \gtrsim N_{e,\rm cr}$ for $t \lesssim 200$ days. From Figure 1 we can estimate that case C should become a valid approximation for $\tau(\text{H}\alpha) \lesssim 3000$, the Balmer continuum should become optically thin for $\tau(\text{H}\alpha) \lesssim 300$, and that the transition from case C to case B should occur for $\tau(\text{H}\alpha) \lesssim 20$.

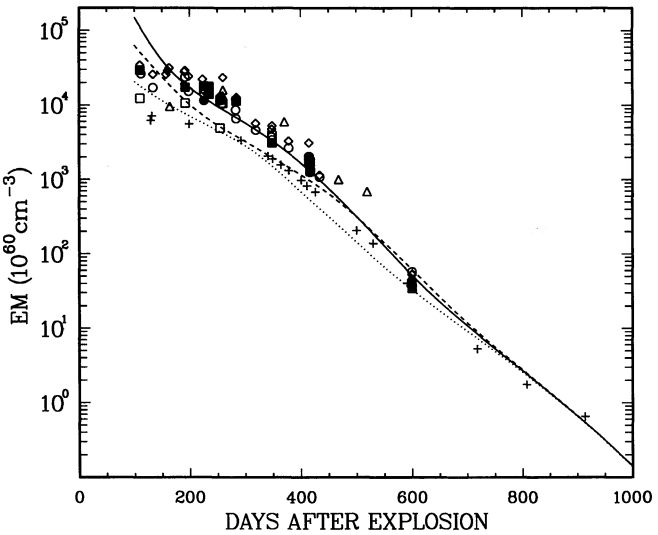

FIG. 2.—Emission measure calculated for model 1 (*solid curves*: $v_{\rm max} = 2500$ km s^{-1} and $\xi_{2,C} = 2$), model 2 (*dashed curves*: $v_{\rm max} = 1500$ km s^{-1} and $\xi_{2,C} = 0$), and model 3 (*dotted curves*: $v_{\rm max} = 3500$ km s^{-1} and $\xi_{2,C} = 0$). Observed emission measure is inferred from case C emissivities (*plus signs*: Hα; *solid circles*: Paα; *open circles*: Paβ; *open squares*: Brα; *solid squares*: Brβ; *diamonds*: Pfγ; *triangles*: Huα). Data references are given in the legend to Fig. 6.

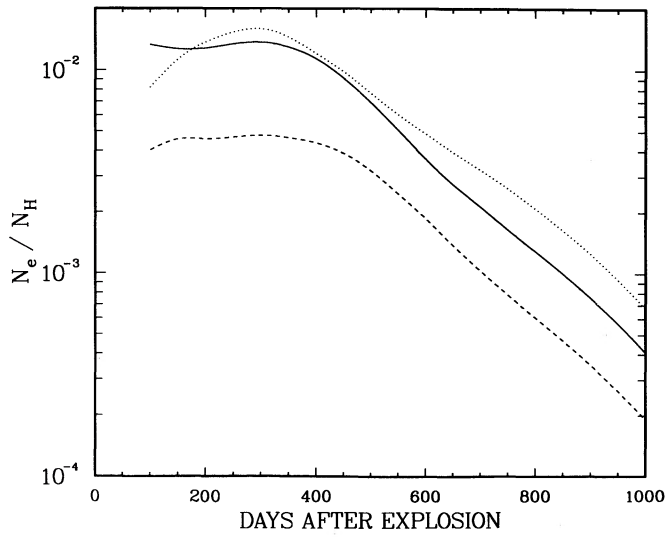

FIG. 3.—Fractional ionization of hydrogen for the three models shown in Fig. 2.

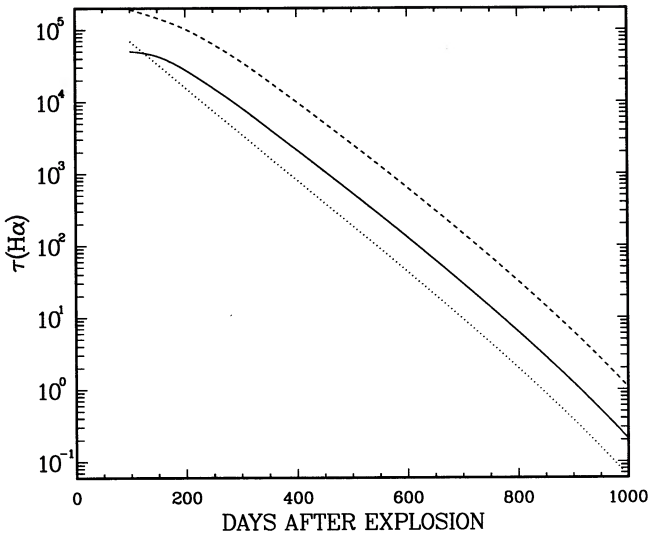

FIG. 4.—Sobolev optical depth of Hα line for the three models shown in Fig. 2.

Referring to Figure 4 (for example, the solid curve representing model 1), we see that these transitions should occur for $t \gtrsim 375$ days, $t \gtrsim 540$ days, and $t \gtrsim 730$ days, respectively.

Figure 5 shows the gamma-ray power deposited in the supernova envelope, $L_\gamma f(t)$ (cf. eqs. [16], [17]), divided by the photon luminosity of all Balmer lines. The Balmer photon luminosity is equal to the total rate of hydrogen recombination throughout the supernova envelope if the Balmer continuum dominates the hydrogen ionization; but it is greater than the rate of hydrogen recombination by a factor of 1.36 if the fast electrons dominate the hydrogen ionization because some of the observed Balmer lines are directly excited by fast electrons. In addition to the three models, results are inferred from observed hydrogen recombination line fluxes by using case C emissivities, ϵ_l, for $\tau(\mathrm{H}\alpha) = 1000$, as was done for Figure 2. The

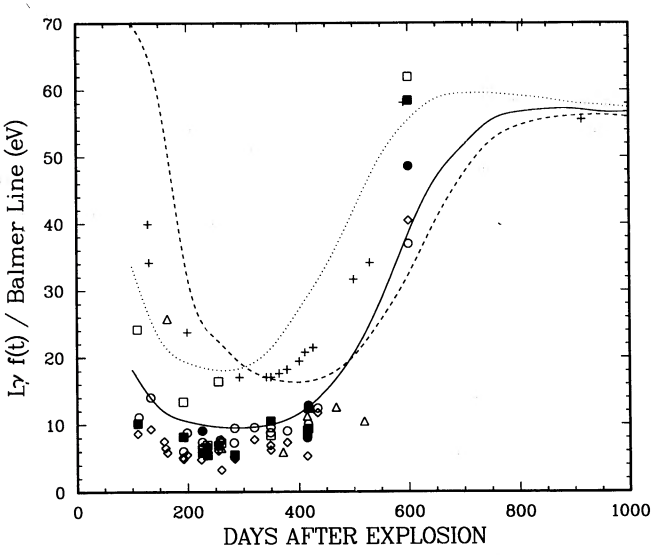

FIG. 5.—Gamma-ray energy used in generating each Balmer line photon. Curves and symbols are the same as those used in Fig. 2.

derived energy per Balmer photon can be written as

$$E_l = \frac{\epsilon_l}{F_l}\left(\sum_{\text{Balmer}} \frac{\epsilon_l}{h\nu_l}\right)^{-1} \tag{20}$$

The behavior of the curves (for example, model 1) can be understood as follows. For $t \lesssim 200$ days, $N_e \gtrsim N_{e,\mathrm{cr}}$ and so N_2 is suppressed by electron impact de-excitation. This in turn suppresses the contribution to N_+ by Balmer continuum photoionization. For $200 \lesssim t \lesssim 375$ days, the gamma-ray energy per ionization is a minimum because Balmer continuum photoionization is fully effective. The fluxes of the infrared lines show that only ~ 8 eV of the fast electron energy is available for each emission of a Balmer photon. Evidently, $\xi_{2,C} \gtrsim 2$ is required to provide such an effective photoionization. For $t \gtrsim 375$ days, the Balmer continuum becomes optically thin; then, the importance of the photoionization from the $n = 2$ level decreases compared with that of the direct ionization by fast electrons. Thus, the efficiency of using the fast electron energy decreases, and finally at $t \sim 800$ days, hydrogen is ionized purely by fast electron collisions and the energy required to emit one Balmer photon increases to ~ 57 eV. (Note that we have assumed that only 50% of the ^{56}Co decay energy is absorbed by hydrogen; the theoretical curves would all decrease by a factor 2 in the case of pure hydrogen.)

Figure 6 shows the predicted fractions of the radioactive energy deposited in the envelope carried by some hydrogen lines, as well as the observed fractions, F_l, of UVOIR luminosity carried by these lines. We selected these lines because they are not blended with other strong lines of heavy elements and they have been observed extensively. For $t \lesssim 650$ days, Hβ was seen as an absorption feature, and we simply took the continuum level on the red side of the line as an upper limit of the line emission.

Model 1 provides about as good a fit to the data as we can find by varying κ, $v_{\max}$, and $\xi_{2,C}$. The results of model 1 are given in Tables 2A, 2B, and 2C for day 377, 494, and 696. As a footnote for each table appear the important parameters and the emissivity for the reference lines, Paβ. The first row and the first column are the lower, l, and upper atomic level, u, of the corresponding transition, respectively. The main body of the table lists the ratios of line intensities relative to that of Paβ. The results agree with the observed light curves of the infrared lines remarkably well, typically within the scatter of the data. For example, models 2 and 3, which lack the extra Balmer continuum flux, do not fit the data. Varying the assumed $v_{\max}$ is tantamount to varying N_{H} or $\tau(\mathrm{H}\alpha)$, and has the effect of scaling the time, as can be seen by comparing the results of models 2 and 3.

Ratios of infrared emission lines originating from the same upper level provide sensitive indicators of optical depth. For example, consider Brα and Paβ, both of which originate from the level $n = 5$. If these lines are optically thin, their ratio must be independent of time. However, both the model calculations and the data show clearly that the light curves of the two lines are different for $t \lesssim 400$ days. From Figure 4 we estimate that for $t \approx 400$ days, $\tau(\mathrm{H}\alpha) \approx 3000$ and, from Figure 1, $\tau(\mathrm{Br}\alpha) \approx 0.03$ and $\tau(\mathrm{Pa}\alpha) \approx 5$. Since $\tau(\mathrm{Pa}\beta) = 0.122\,\tau(\mathrm{Pa}\alpha) \approx 0.6$ (cf. eq. [1]), we see that for $t \lesssim 400$ days, the emissivity of Paβ is suppressed because of the splitting $\mathrm{Pa}\beta \rightarrow \mathrm{Pa}\alpha + \mathrm{Br}\alpha$. That explains the plateau of the Paβ light curve for $t \lesssim 400$ days seen in model 1 and the data.

A similar comparison can be made between Huα and Brγ,

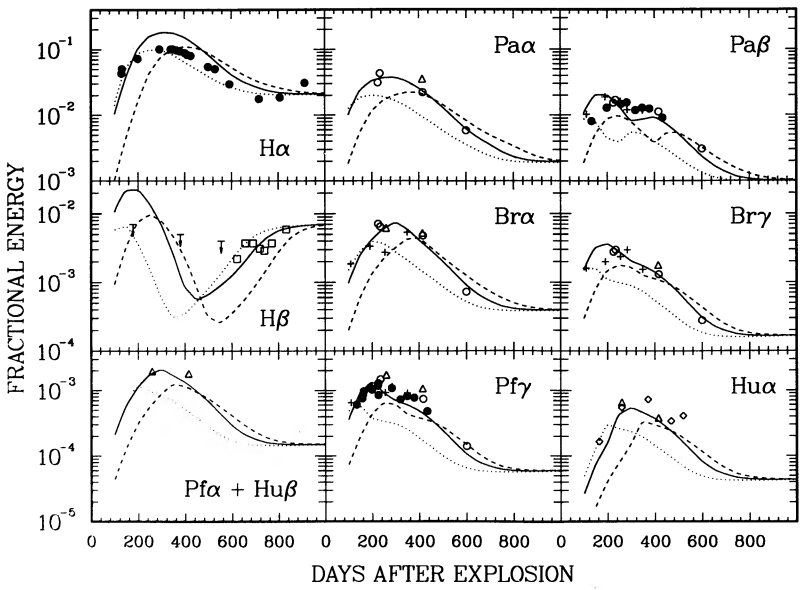

FIG. 6.—Fraction of UVOIR luminosity carried by hydrogen lines. The observed data are marked as round disks observed by CTIO (Phillips & Williams 1991), circles by ESO (Oliva et al. 1987, 1989), triangles by KAO (Wooden 1989), plus signs by AAO (Miekle et al. 1989), squares by SAO (Menzies 1990), and diamonds by Aitken et al. (1988) and Aitken (1990).

both of which originate from the level $n = 7$. According to Figure 1, $\tau(\mathrm{Hu}\alpha) \gtrsim 1$ for $\tau(\mathrm{H}\alpha) \gtrsim 2 \times 10^4$, or $t \lesssim 230$ days, according to Figure 4. Indeed, we see that the brightness of Huα continued to rise until that time and declined thereafter as Huα became optically thin. On the other hand, Brγ has a lower optical depth than Huα [$\tau(\mathrm{Br}\gamma) = 0.034\tau(\mathrm{Br}\alpha)$], and so Br$\gamma$ reaches its peak intensity earlier than Huα.

It is also reassuring that Hβ emerged at $t \sim 600$ days, for which $\tau(\mathrm{H}\alpha) \approx 100$. This behavior is just as expected, according to Figure 1.

The shape of the observed light curve of Hα also agrees fairly well with model 1. One major discrepancy remains, however: the observed intensity of Hα is consistently less than expected by a factor ~ 2.

4. DISCUSSION

We can account for the observed light curves of the hydrogen recombination lines of SN 1987A with a fairly simple homogeneous model. The fit to the data provides three major constraints.

First, roughly half of the total gamma-ray luminosity must be deposited in hydrogen-rich gas in the envelope. Since the energy deposition is roughly proportional to the number of (bound and free) electrons, this conclusion requires that roughly one-third of the total mass illuminated by the gamma rays is hydrogen.

Second, for $t \lesssim 400$ days, hydrogen must be ionized primarily from the $n = 2$ level by Balmer continuum photons. The production rate of H^+ by this mechanism must be approximately 5 times the rate due to ionization from the ground state by fast electrons. This mechanism requires a source of Balmer continuum that is roughly twice that provided by the two-photon decay of the $n = 2$ level.

Third, the local hydrogen density, $N_{\mathrm{H}}(t)$, is determined by the light curves of infrared lines. Since model 1 provides a good fit to the data, $\tau(\mathrm{H}\alpha)(t)$ is given by the solid curve of Figure 4, and $N_{\mathrm{H}}(t)$ then follows from equation (8). $N_{\mathrm{H}}(t)$ is related to the total hydrogen mass, M_{H}, expansion velocity, $v_{\max}$, and filling factor, f_{H}, by equation (15). The observed line widths indicate that $v_{\max} \approx 2500$ km s^{-1}, and we know that M_{H} must be a few solar masses in order to satisfy the first constraint. Therefore, we can conclude that the hydrogen must have a filling factor $f_{\mathrm{H}} \sim 1$.

Given this model, we can infer the emission measure and the ionized fraction of the emitting hydrogen as a function of time (cf. Figs. 2 and 3).

Our model results are insensitive to the assumed temperature, provided that thermal electron impact excitation is negligible compared to radiative cascade. That will be true provided that $T \lesssim 6000$ K. We have verified this by calculating models with $T = 5000$ K, which give the same results as those with $T = 3000$ K, holeding the other parameters constant.

Of course, the models presented here must be an oversimplification of the actual situation. Surely, there must be spatial variations in N_{H}. One could easily make more complicated models allowing for such variations; they would be linear superpositions of the models we have shown, with different time scales. However, the data available to us are not of sufficient quality to warrant such an exercise.

There are two outstanding problems. The first is the source of the Balmer continuum photons. We have assumed that this source has the same exponential decay rate as the ^{56}Co. We presume that these photons are produced by the helium and the metals that are mixed (macroscopically) with the hydrogen. When fast electrons are stopped by helium and metals, much of the energy is emitted in 912–2000 Å photons, which are then converted to Balmer continuum photon emission of helium (Kozma & Fransson 1991) or by fluorescence with metals such as Fe I and Fe II (Xu & McCray 1991b). In fact, Kozma & Fransson (1991) estimated the ionizing flux of the Balmer continuum by use of detailed hydrodynamical models of SN 1987A. Their estimated flux is almost exactly equal to the extra UV radiation field that we required for Model 1 to fit the data. We emphasize that the absence of observed Balmer continuum is the spectrum of SN 1987A does not constrain the intensity of the Balmer continuum that may be present in the line-emitting

TABLE 2A

RECOMBINATION LINE RATIOS: DAY 377

λ	2	3	4	5	6	7	8	9	10	11	12	13	14
15.....	5.77 (−2)	5.30 (−2)	2.28 (−2)	1.18 (−2)	6.84 (−3)	4.31 (−3)	2.89 (−3)	2.02 (−3)	1.46 (−3)	1.09 (−3)	8.21 (−4)	6.21 (−4)	4.51 (−4)
14.....	5.50 (−2)	6.08 (−2)	2.61 (−2)	1.35 (−2)	7.84 (−3)	4.94 (−3)	3.30 (−3)	2.31 (−3)	1.66 (−3)	1.23 (−3)	9.08 (−4)	6.47 (−4)	
13.....	5.22 (−2)	7.17 (−2)	3.08 (−2)	1.59 (−2)	9.22 (−3)	5.80 (−3)	3.87 (−3)	2.69 (−3)	1.92 (−3)	1.39 (−3)	9.71 (−4)		
12.....	4.91 (−2)	8.62 (−2)	3.71 (−2)	1.91 (−2)	1.11 (−2)	6.94 (−3)	4.61 (−3)	3.18 (−3)	2.23 (−3)	1.52 (−3)			
11.....	4.70 (−2)	1.09 (−1)	4.68 (−2)	2.41 (−2)	1.39 (−2)	8.68 (−3)	4.72 (−3)	3.87 (−3)	2.56 (−3)				
10.....	4.42 (−2)	1.39 (−1)	5.99 (−2)	3.08 (−2)	1.77 (−2)	1.10 (−2)	7.09 (−3)	4.52 (−3)					
9.....	4.18 (−2)	1.86 (−1)	8.03 (−2)	4.10 (−2)	2.34 (−2)	1.42 (−2)	8.67 (−3)						
8.....	3.90 (−2)	2.58 (−1)	1.12 (−1)	5.66 (−2)	3.17 (−2)	1.82 (−2)							
7.....	3.61 (−2)	3.76 (−1)	1.65 (−1)	8.20 (−2)	4.32 (−2)								
6.....	3.33 (−2)	5.86 (−1)	2.65 (−1)	1.24 (−1)									
5.....	3.27 (−2)	1.00 (0)	5.06 (−1)										
4.....	1.31 (−1)	3.00 (0)											
3.....	1.75 (1)												

NOTE.—$t = 377^{d}$, $\tau(\mathrm{H}\alpha) = 3000$, $T = 3000$ K, $N_e = 3.03 \times 10^{7}$ cm^{-3}, $\epsilon(5\text{–}3) = 1.01 \times 10^{-25}$ ergs cm^{3} s^{-1}.

TABLE 2B

RECOMBINATION LINE RATIOS: DAY 494

λ	2	3	4	5	6	7	8	9	10	11	12	13	14
15.....	9.63 (−2)	3.85 (−2)	1.65 (−2)	8.53 (−3)	4.96 (−3)	3.13 (−3)	2.09 (−3)	1.47 (−3)	1.06 (−3)	7.89 (−4)	5.96 (−4)	4.50 (−4)	3.27 (−4)
14.....	1.06 (−1)	4.52 (−2)	1.94 (−2)	9.99 (−3)	5.80 (−3)	3.66 (−3)	2.44 (−3)	1.71 (−3)	1.23 (−3)	9.07 (−4)	6.72 (−4)	4.79 (−4)	
13.....	1.20 (−1)	5.53 (−2)	2.37 (−2)	1.22 (−2)	7.09 (−3)	4.46 (−3)	2.97 (−3)	2.07 (−3)	1.48 (−3)	1.07 (−3)	7.46 (−4)		
12.....	1.32 (−1)	6.78 (−2)	2.90 (−2)	1.49 (−2)	8.66 (−3)	5.43 (−3)	3.61 (−3)	2.49 (−3)	1.75 (−3)	1.19 (−3)			
11.....	1.46 (−1)	8.64 (−2)	3.69 (−2)	1.90 (−2)	1.10 (−2)	6.85 (−3)	4.51 (−3)	3.05 (−3)	2.02 (−3)				
10.....	1.56 (−1)	1.12 (−1)	4.79 (−2)	2.46 (−2)	1.42 (−2)	8.77 (−3)	5.67 (−3)	3.62 (−3)					
9.....	1.62 (−1)	1.53 (−1)	6.49 (−2)	3.32 (−2)	1.89 (−2)	1.15 (−2)	7.01 (−3)						
8.....	1.59 (−1)	2.16 (−1)	9.16 (−2)	4.64 (−2)	2.60 (−2)	1.49 (−2)							
7.....	1.51 (−1)	3.25 (−1)	1.37 (−1)	6.79 (−2)	3.58 (−2)								
6.....	1.39 (−1)	5.31 (−1)	2.20 (−1)	1.03 (−1)									
5.....	1.25 (−1)	1.00 (0)	3.90 (−1)										
4.....	1.17 (−1)	2.55 (0)											
3.....	1.60 (1)												

NOTE.—$t = 494^{d}$, $\tau(\mathrm{H}\alpha) = 594$, $T = 3000$ K, $N_e = 8.01 \times 10^{6}$ cm^{-3}, $\epsilon(5\text{–}3) = 1.07 \times 10^{-25}$ ergs cm^{3} s^{-1}.

TABLE 2C

RECOMBINATION LINE RATIOS: DAY 696

λ	2	3	4	5	6	7	8	9	10	11	12	13	14
15.....	1.43 (−1)	4.46 (−2)	1.91 (−2)	9.87 (−3)	5.74 (−3)	3.62 (−3)	2.42 (−3)	1.70 (−3)	1.23 (−3)	9.13 (−4)	6.89 (−4)	5.21 (−4)	3.78 (−4)
14.....	1.71 (−1)	5.32 (−2)	2.28 (−2)	1.18 (−2)	6.83 (−3)	4.30 (−3)	2.88 (−3)	2.01 (−3)	1.45 (−3)	1.07 (−3)	7.91 (−4)	5.64 (−4)	
13.....	2.07 (−1)	6.48 (−2)	2.77 (−2)	1.43 (−2)	8.30 (−3)	5.22 (−3)	3.48 (−3)	2.42 (−3)	1.73 (−3)	1.25 (−3)	8.75 (−4)		
12.....	2.53 (−1)	7.96 (−2)	3.41 (−2)	1.75 (−2)	1.02 (−2)	6.38 (−3)	4.23 (−3)	2.92 (−3)	2.05 (−3)	1.40 (−3)			
11.....	3.14 (−1)	1.00 (−1)	4.27 (−2)	2.20 (−2)	1.27 (−2)	7.93 (−3)	5.22 (−3)	3.53 (−3)	2.34 (−3)				
10.....	3.98 (−1)	1.28 (−1)	5.47 (−2)	2.80 (−2)	1.61 (−2)	1.00 (−2)	6.46 (−3)	4.12 (−3)					
9.....	5.16 (−1)	1.70 (−1)	7.22 (−2)	3.69 (−2)	2.11 (−2)	1.28 (−2)	7.80 (−3)						
8.....	6.85 (−1)	2.33 (−1)	9.89 (−2)	5.01 (−2)	2.81 (−2)	1.61 (−2)							
7.....	9.34 (−1)	3.39 (−1)	1.43 (−1)	7.10 (−2)	3.74 (−2)								
6.....	1.30 (0)	5.38 (−1)	2.22 (−1)	1.04 (−1)									
5.....	1.79 (0)	1.00 (0)	3.88 (−1)										
4.....	2.16 (0)	2.64 (0)											
3.....	2.02 (1)												

NOTE.—$t = 696^{d}$, $\tau(\mathrm{H}\alpha) = 32$, $T = 3000$ K, $N_e = 8.80 \times 10^{5}$ cm^{-3}, $\epsilon(5\text{–}3) = 8.19 \times 10^{-26}$ ergs cm^{3} s^{-1}.

region, because such radiation can be absorbed in the outer envelope by a forest of resonance lines of Fe I, Fe II (Xu & McCray 1991b).

The second problem is more puzzling. We have not been able to identify a physical mechanism to account for the fact that Hα is lower than expected by a factor ~ 2. This puzzle cannot be solved by considering models with density distributions. As shown in Figure 6, changing density is equivalent to changing the time scale of the theoretical light curves, but the ratios between the luminosities of different lines are nearly fixed for given N_H. We have considered several other possibilities and found them all wanting. For example, the continuum absorption optical depths due to free-free absorption and H^- absorption fall short by orders of magnitude. An obvious possibility is absorption by dust within the supernova envelope. We consider this explanation unlikely, however, because one would expect the dust (or any other continuum mechanism) preferentially to absorb the emission from the far side of the envelope, causing a blueshift of the line centroid. This effect was seen clearly in the dust formation event that occurred at $t \approx 550$ days (Danziger et al. 1991), but was not seen earlier.

Electron impact de-excitation of the $n = 3$ level and photoionization from $n = 3$ by photons in the Paschen continuum also fail by orders of magnitude. Perhaps Hα is suppressed by some mechanism that strongly absorbs Lyβ. One obvious candidate, the resonance fluorescence of O I, can be ruled out, however, because the photon luminosity of the resulting O I $\lambda 1.129$ μm is substantially less than the missing luminosity of Hα photons. One remaining possibility is a stronger resonance fluorescence of Lyβ with some other metallic line that we have not yet identified.

With the exception of the Hα problem, we have developed a theory for development of the hydrogen emission line spectrum of SN 1987A that agrees remarkably well with the observations and enables us to infer the physical conditions within the emission-line region with considerable confidence.

Finally, we note that there is evidence for optically thick recombination line emission in other important astrophysical systems. For example, in star-forming regions, the strength of infrared recombination lines exceeds the value that would be expected from the estimated ionizing photon luminosity and case B recombination line theory (Thompson 1987). Likewise, there is evidence that the Balmer series is optically thick in the spectra of active galactic nuclei (cf. Drake & Ulrich 1980). However, the estimated temperatures and densities of the emitting gas in those systems are substantially greater than those in SN 1987A. Therefore, different physical processes, such as electron impact excitation from $n = 2$, 3, etc., will dominate in the formation of the recombination spectra of those systems. Moreover, models for such systems will be sensitive to the escape probabilities, which are more uncertain because the geometry and velocity distribution of the gas are less well-defined than in SN 1987A.

This work was supported in part by NSF grant AST 87-22126 and by grant NAGW-766 under the NASA Astrophysical Theory Program at the University of Colorado.

REFERENCES

Aitken, D. K. 1990, private communication
Aitken, D. K., Smith, C. H., James, S. D., Roche, P. F., Hyland, A. R., & McGregor, P. J. 1988, MNRAS, 235, 19P
Aller, L. H., Baker, J. G., & Menzel, D. H. 1939, ApJ, 89, 587
Brocklehurst, M. 1971, MNRAS, 153, 471
Castor, J. 1970, MNRAS, 149, 111
Danziger, I. J., Lucy, L. B., Bouchet, P., & Gouiffes, C. 1991, in Supernovae, ed. S. E. Woosley (New York: Springer), 69
Drake, S. A., & Ulrich, R. K. 1980, ApJS, 42, 351
Dwek, E. 1991, in Supernovae ed. S. E. Woosley (New York: Springer), 54
Grandi, S. A. 1980, ApJ, 238, 10
Hummer, D. G., & Storey, P. J. 1987, MNRAS, 224, 801
Johnson, L. C. 1972, ApJ, 174, 227
Kozma, C., & Fransson, C. 1991, ApJ, submitted
Menzies, J. W. 1990, private communication
Miekle, W. P. S., Allen, D. A., Spyromilio, J., & Varani, G. 1989, MNRAS, 238, 193
Mihalas, D. 1978, Stellar Atmospheres (2d ed.; San Francisco: W. H. Freeman Co.)
Nomoto, K., Shigeyama, T., Kumagai, S., & Yamaoka, H. 1991, in Supernovae, ed. S. E. Woosley (New York: Springer), 176
Nussbaumer, H., & Schmütz, W. 1984, A&A, 138, 495
Oliva, E., Moorwood, A. F. M., & Danziger, I. J. 1987, Messenger, 50, 18
———. 1989, in 22nd ESLAB Symposium, Infrared Spectroscopy in Astronomy (ESA SP-290), ed. B. H. Kaldeich (Paris: European Space Agency), 375
Osterbrock, D. E. 1989, Astrophysics of Gaseous Nebulae and Active Galactic Nuclei (Mill Valley, CA: University Science Books)
Phillips, M. M., & Williams, R. E. 1991, in Supernovae, ed. S. E. Woosley (New York: Springer), 36
Seaton, M. F. 1959, ApJ, 119, 81
Shull, J. M., & van Steenberg, M. E. 1985, ApJ, 298, 268
Sobolev, V. 1960, Moving Envelopes of Stars (Cambridge, Mass.: Harvard Univ. Press)
Thompson, R. I. 1987, ApJ, 312, 784
Varani, G. F., Meikle, W. P. S., Spyromilio, J., & Allen, D. A. 1990, MNRAS, 245, 570
Wooden, D. H. 1989, Ph.D. thesis, University of California at Santa Cruz
Woosley, S. E. 1988, ApJ, 330, 218
Xu, Y. 1989, Ph.D. thesis, University of Colorado at Boulder
Xu, Y., & McCray, R. 1991a, ApJ, 375, 190
———. 1991b, in Supernovae, ed. S. E. Woosley (New York: Springer), 444